Inorg. Chem. **2003**, *42*, 5005–5014

Controlled Reactions on a Copper Surface: Synthesis and Characterization of Nanostructured Copper Compound Films

Weixin Zhang, Xiaogang Wen, and Shihe Yang*

Department of Chemistry and Institute of Nano Science and Technology, The Hong Kong University of Science and Technology, Clear Water Bay, Kowloon, Hong Kong

Received April 21, 2003

We report the synthesis of nanostructured copper compound films on a copper surface under mild conditions. A series of low-dimensional structures including $Cu(OH)_2$ fibers and scrolls, CuO sheets and whiskers, and $Cu_2(OH)_2CO_3$ rods have been successfully grown on the copper surfaces at ambient temperature and pressure. Most of the structures are phase-pure single crystallites. The films were formed by the direct oxidation of copper in aqueous solutions of NaOH with an oxidant $(NH_4)_2S_2O_8$. The evolution of the ultrafine structures as a function of the reaction conditions has been revealed, from fibers of $Cu(OH)_2$ to scrolls of $Cu(OH)_2$ to sheets or whiskers of CuO. By replacing NaOH with $NaHCO_3$ in the synthesis, square/rectangular rod arrays of $Cu_2(OH)_2CO_3$ were obtained. The controlled reactions allow the large-scale, template-free, cost-effective synthesis of copper compound films with ordered, uniform, stable, ultrafine structures.

Introduction

In recent years, there has been considerable effort in the fabrication of ordered nanostructures, which are essential to the realization of high-performance devices.[1−9] In particular, carbon nanotubes[10] and metallic (Ni,[11] Bi,[12] Ag,[13] etc.) and semiconductor (ZnO,[14] Bi_2Te_3,[15] Cu_2S,[16] etc.) nanowires have been successfully aligned in arrays. These nanotube and nanowire arrays have aroused great interest because of their importance in the exploration of quantum size/dimension effects and because of possible applications in electronics, mechanics, and biomedicine.

Porous anodic aluminum oxide[17] and polymer membranes (e.g., polycarbonate)[18] have been used as templates to prepare ordered metal and semiconductor nanowire arrays with controlled dimensions. One of the problems with this technique is that the nanowires are prone to aggregation when the templates are etched away.[19] Lithography,[20] epitaxial electrodeposition,[21] and chemical vapor deposition (CVD)[11,22] have also been used to fabricate supported nanostructured films. Recently, Vayssieres et al.[23] reported the aqueous chemical growth of oriented 3D crystalline iron (III) oxide nanorod arrays and ZnO microrod/tube arrays at 90−100 °C. Posttreatment at higher temperatures may be required to improve the crystallinity and morphological quality of the nano- or microstructures.

* Corresponding author. E-mail: chsyang@ust.hk.

(1) Pileni, M. P. *J. Phys. Chem. B* **2001**, *105*, 3358.
(2) Murray, C. B.; Kagan, C. R.; Bawendi, M. G. *Science* **1995**, *270*, 1335.
(3) Soulantica, K.; Maisonnat, A.; Fromen, M. C.; Casanove, M. J.; Lecante, P.; Chaudret, B. *Angew. Chem., Int. Ed.* **2001**, *40*, 448.
(4) Brown, L. O.; Hutchison, J. E. *J. Am. Chem. Soc.* **1999**, *121*, 882.
(5) Tripp, S. L.; Pusztay, S. V.; Ribbe, A. E.; Wei, A. *J. Am. Chem. Soc.* **2002**, *124*, 7914.
(6) Yonezawa, T.; Onoue, S.; Kimizuka, N. *Adv. Mater.* **2001**, *13*, 140.
(7) Hong, B. H.; Lee, J. Y.; Lee, C.-W.; Kim, J. C.; Bae, S. C.; Kim, K. S. *J. Am. Chem. Soc.* **2001**, *123*, 10748.
(8) Zhang, Z.; Gekhtman, D.; Dresselhaus, M. S.; Ying, J. Y. *Chem. Mater.* **1999**, *11*, 1659.
(9) Yin, A. J.; Li, J.; Jian, W.; Bennett, A. J.; Xu, J. M. *Appl. Phys. Lett.* **2001**, *79*, 1039.
(10) (a) Li, W. Z.; Xie, S. S.; Qian, L. X.; Chang, B. H.; Zou, B. S.; Zhou, W. Y.; Zhao, R. A.; Wang, G. *Science* **1996**, *274*, 1701. (b) Thostenson, E. T.; Ren, Z.; Chou, T. W. *Comput. Sci. Technol.* **2001**, *61*, 1899. (c) Hu, W.; Gong, D.; Chen, Z.; Yuan, L.; Saito, K.; Grimes, C. A.; Kichambare, P. *Appl. Phys. Lett.* **2001**, *79*, 3083.
(11) Nielsch, K.; Wehrspohn, R. B.; Barthel, J.; Kirschner, J.; Gösele, U.; Fischer, S. F.; Kronmüller, H. *Appl. Phys. Lett.* **2001**, *79*, 1360.
(12) Zhang, Z.; Sun, X.; Dresselhaus, M. S.; Ying, J. Y.; Heremans, J. P. *Appl. Phys. Lett.* **1998**, *73*, 1589.
(13) Hong, B. H.; Bae, S. C.; Lee, C.-W.; Jeong, S.; Kim, K. S. *Science* **2001**, *294*, 348.
(14) Huang, M. H.; Mao, S.; Feick, H.; Yan, H.; Wu, Y.; Kind, H.; Weber, E.; Russo, R.; Yang, P. *Science* **2001**, *292*, 1897.
(15) Prieto, A. L.; Sander, M. S.; Martin-Gonzalez, M. S.; Gronsky, R.; Sands, T.; Stacy, A. M. *J. Am. Chem. Soc.* **2001**, *123*, 7160.
(16) Chen, J.; Deng, S. Z.; Xu, N. S.; Wang, S.; Wen, X.; Yang, S.; Yang, C.; Wang, J.; Ge, W. *Appl. Phys. Lett.* **2002**, *80*, 3620.
(17) Martin, C. R. *Science* **1994**, *266*, 1961.
(18) Hulteen, J. C.; Martin, C. R. *J. Mater. Chem.* **1997**, *7*, 1075.
(19) (a) Sapp, S. A.; Lakshmi, B. B.; Martin, C. R. *Adv. Mater.* **1999**, *11*, 402. (b) Cepak, V. M.; Martin, C. R. *J. Phys. Chem. B* **1998**, *102*, 9985.
(20) Xia, Y.; Rogers, J. A.; Paul, K. E.; Whitesides, G. M. *Chem. Rev.* **1999**, *99*, 1823.
(21) Liu, R.; Vertegel, A. A.; Bohannan, E. W.; Sorenson, T. A.; Switzer, J. A. *Chem. Mater.* **2001**, *13*, 508.
(22) Nigro, R. L.; Malandrino, G.; Fragalà. I. L. *Chem. Mater.* **2001**, *13*, 4402.

10.1021/ic0344214 CCC: $25.00
Published on Web 07/18/2003

In this paper, we exploit the concept of nanostructural engineering on a metal surface through a solution chemical route. This stems from our earlier finding that Cu_2S nanowires could be grown in uniform arrays on a copper surface.[24] A unique appeal of this concept lies in the natural device structure of semiconductor nanowires arrayed on a metal surface, which could be directly used in areas such as field emission and chemical/biochemical sensing. Here, we present a simple, mild, template-free method to prepare large arrays of ordered ultrafine structures, from fibers and scrolls of $Cu(OH)_2$, sheets and whiskers of CuO, and rods of $Cu_2(OH)_2CO_3$, on copper surfaces. The key to the synthesis of such structures on copper is the control of the reaction conditions in solution at ambient temperature and pressure.

The target copper compound materials are interesting by themselves. For example, the magnetic properties of layer-structured hydroxide compounds can be modified significantly by anion exchange to form $M_2(OH)_3X$ (M = Cu, Co, Ni; X = intercalated anion, e.g., NO_3^-, alkane carboxylates, etc.).[25] Cupric oxide as a dehydration product of $Cu(OH)_2$ is of considerable interest owing to its roles in catalysis, metallurgy, and high-T_c superconductors.[26−28] It is also well known in the battery community as a positive electrode material in primary commercial CuO/Li cells with a discharge voltage between 1.4 and 1.0 V.[29] Nanocrystals of the semiconducting CuO are relatively unexplored compared to the II−VI and III−V semiconductors.[30,31]

The synthesis of these copper compound materials is commonly accomplished in solution using Cu(II) salts. Much work has been done by Matijević and co-workers on the synthesis of needlelike crystalline $Cu(OH)_2$, amorphous $Cu_2(OH)_2CO_3$ ball-shaped microparticles, and related copper compounds by homogeneous precipitation.[32] The growth of single crystals of $Cu(OH)_2$ by dipping a high-purity copper ribbon into a solution of ammonia (12.5%) and acetone (12.5%) at 277 K for 3 weeks has allowed Oswald et al.[33] to refine the crystal structure of $Cu(OH)_2$. Bulk CuO can be easily obtained by the hydrometallurgical conversion of $Cu(OH)_2$ or $Cu(NH_3)_4CO_3$ at elevated temperature and high pH.[34,35] Nanoparticles of CuO have been prepared by a metal organic deposition technique[36] and have been assembled on SiO_2 by spin coating.[37] An electrochemical route,[38] a sol−gel-like dip technique,[39] and Langmuir−Blodgette deposition [40] have been used to prepare CuO nanoparticle thin films. Recently, efforts have been spent on the synthesis of 1D materials of CuO. For example, CuO rods have been obtained by grinding a mixture of $CuCl_2$ and NaOH in a nonionic surfactant.[41] Simply heating a copper grid at 400 °C in air has been demonstrated to produce CuO wires with mixed phases.[42]

Our synthetic method consists of controlled surface oxidation on copper substrates in alkaline aqueous solutions (NaOH or $NaHCO_3$) with $(NH_4)_2S_2O_8$. The copper substrates are used not only as a source of copper but also as a support for the copper compound films. In the following text, the synthesis, structures, and morphologies of the films obtained under different conditions are described, and possible growth mechanisms are discussed.

Experimental Section

Materials and Methods. Stock solutions of sodium hydroxide (10 mol dm^{-3}), sodium hydrogen carbonate (1.0 mol dm^{-3}), and ammonium persulfate (1.0 mol dm^{-3} and 0.20 mol dm^{-3}) were prepared by dissolving NaOH (99.0−100.5%, Riedel−de Haën), $NaHCO_3$ (99.7−100.3%, BDH), and $(NH_4)_2S_2O_8$ (98%, Riedel−de Haën) in deionized water, respectively, and stored in glass bottles. High-purity copper foils (99.99%, Aldrich) were used as received.

A typical synthesis of $Cu(OH)_2$ and CuO on copper foils was performed as follows. An aqueous solution was prepared in a 100-mL glass bottle by mixing 4.0 mL of the NaOH solution, 2.0 mL of a $(NH_4)_2S_2O_8$ solution (1.0 M), and 9.0 mL of water. The total solution volume was kept at 15 mL. A piece of copper foil ($10 \times 3.0 \times 0.25$ mm^3), which had been ultrasonically cleaned in acetone and then in deionized water, was immersed in the solution. A few minutes later, a faint blue color appeared on the copper foil surface, and the initial colorless solution became increasingly blue. In 15 min, a light-blue film covered the copper foil surface. When the

(23) (a) Vayssieres, L.; Beermann, N.; Lindquist, S.-E.; Hagfeldt, A. *Chem. Mater*. **2001**, *13*, 233. (b) Vayssieres, L.; Keis, K.; Lindquist, S.-E.; Hagfeldt, A. *J. Phys. Chem. B* **2001**, *105*, 3350. (c) Vayssieres, L.; Keis, K.; Hagfeldt, A.; Lindquist, S.-E. *Chem. Mater*. **2001**, *13*, 4395.

(24) (a) Wang, S.; Yang, S. *Chem. Phys. Lett*. **2000**, *322*, 567. (b) Wang S.; Yang, S. *Adv. Mater. Opt. Electron.* **2000**, *10*, 39. (c) Wang, S.; Yang, S. *Mater. Sci. Eng., C* **2001**, *16*, 37. (d) Wang, S.; Yang, S.; Dai, Z. R.; Wang, Z. L. *Phys. Chem. Chem. Phys.* **2001**, *3*, 3750. (e) Wang, S.; Yang, S. *Chem. Mater*. **2001**, *13*, 4794. (f) Wang, N.; Fung, K. K.; Wang, S.; Yang, S. *J. Cryst. Growth* **2001**, *233*, 226.

(25) (a) Yamanaka, S.; Sako, T.; Seki, K.; Hattori, M. *Solid State Ionics* **1992**, *53−56*, 527. (b) Marangoni, R.; Bubniak, G. A.; Cantão, M. P.; Abbate, M.; Schreiner, W. H.; Wypych, F. *J. Colloid Interface Sci*. **2001**, *240*, 245. (c) Poul, L.; Jouini, N.; Fiévet, F. *Chem. Mater*. **2000**, *12*, 3123. (d) Fujita, W.; Awaga, K. *J. Am. Chem. Soc*. **1997**, *119*, 4563. (e) Kurmoo, M. *Chem. Mater*. **1999**, *11*, 3370.

(26) (a) Reitz, J. B.; Solomon, E. I. *J. Am. Chem. Soc*. **1998**, *120*, 11467. (b) Larsson, P.; Andersson, A. *J. Catal*. **1998**, *179*, 72. (c) Chikán, V.; Molnár, Á.; Balázsik, K. *J. Catal*. **1999**, *184*, 134.

(27) Raveau, B.; Michel, C.; Herview, M.; Groult, D. *Crystal Chemistry of High-T_c Superconducting Copper Oxides*; Springer-Verlag: Berlin, 1991.

(28) Poole, C. P.; Datta, T.; Farach, H. A.; Rigney, M. M.; Sanders, C. R. *Copper Oxide Superconductors*; Wiley & Sons: New York, 1988.

(29) (a) Débart, A.; Dupont, L.; Poizot, P.; Leriche, J.-B.; Tarascon, J. M. *J. Electrochem. Soc*. **2001**, *148*, A1266. (b) Hibble, S. J.; Malitesta, C.; Dickens, P. G. *Solid State Ionics* **1990**, *39*, 289.

(30) (a) Borgohain, K.; Singh, J. B.; Rao, M. V. R.; Shripathi, T.; Mahamuni, S. *Phys. Rev.* B **2000**, *61*, 11093. (b) Borgohain, K.; Mahamuni, S. *J. Mater. Res*. **2002**, *17*, 1220.

(31) Palker, V. R.; Ayyub, P.; Chattopadhyay, S.; Multani, M. *Phys. Rev. B* **1996**, *53*, 2167.

(32) (a) Kratohvil S.; Matijević, E. *J. Mater. Res*. **1991**, *6*, 766. (b) Rodríguez-Clemente, R.; Serna, C. J.; Ocaña, M.; Matijević, E. *J. Crystal Growth* **1994**, *143*, 277. (c) Lee, S. H.; Her, Y. S.; Matijević, E. *J. Colloid Interface Sci*. **1997**, *186*, 193.

(33) Oswald, H. R.; Reller, A.; Schmalle H. W.; Dubler, E. *Acta Crystallogr., Sect. C* **1990**, *46*, 2279.

(34) Richardson, H. W. *Handbook of Copper Compounds and Applications*; Marcel Dekker: New York, 1997; p 58.

(35) Carnes, C. L.; Stipp, J.; Klabunde, K. J. *Langmuir* **2002**, *18*, 1352.

(36) Galembeck, A.; Alves, O. L. *Synth. Met*. **1999**, *102*, 1238.

(37) Brookshier, M. A.; Chusuei, C. C.; Goodman, D. W. *Langmuir* **1999**, *15*, 2043.

(38) Reetz, M. T.; Helbig, W. *J. Am. Chem. Soc*. **1996**, *116*, 7401.

(39) Ray, S. C. *Sol. Energy Mater. Sol. Cells* **2001**, *68*, 307.

(40) Schurr, M.; Seidl, M.; Brugge, A.; Voit, H. *Thin Solid Films* **1999**, *342*, 266.

(41) (a) Wang, W.; Zhan, Y.; Wang, G. *Chem. Commun*. **2001**, 727. (b) Wen, X. G.; Zhang, W. X.; Yang, S. H.; Dai, Z. R.; Wang, Z. L. *Nano Lett*. **2002**, *2*, 1397.

(42) (a) Suzuki, H.; Fukuzawa, N.; Tanigaki, T.; Sato, T. Kido, O.; Kimura, Y.; Kaito, C. *J. Cryst. Growth* **2002**, *244*, 168. (b) Jiang, X.; Herricks, T.; Xia, Y. *Nano Lett*. **2002**, *2*, 133.

Table 1. Reaction Conditions and Results for the Oxidation of a Copper Foil ($10 \times 3.0 \times 0.25$ mm^3) in Alkaline Solutions

pH value of the mixture solution	molar ratio of NaOH to $(NH_4)_2S_2O_8$	concentration of NaOH (M)	product composition		reaction time (h)	product morphology
			precipitate	film		
8−10	0.5−10	0.02−0.12	$Cu_4(SO_4)(OH)_6$		>2.0	spindlelike
10−13	2.0−4.0	0.12−0.25	CuO		>4.0	sheetlike
13−14	4.0−25	0.25−1.0		CuO	>0.5	sheetlike
>14	5.0−50	1.0−5.0		CuO	>10	sheetlike
>14	5.0−50	5.0−7.0		CuO	>1.5	sheet/whisker
>14	10−40	1.0−2.0		$Cu(OH)_2$	0.1−9.0	fiber
>14	10−40	2.0−5.5		$Cu(OH)_2$	1.0−1.5	scroll

Table 2. Reaction Conditions and Results for the Growth of $Cu_2(OH)_2CO_3$ Rods

sample no.	molar ratio of $NaHCO_3$ to $(NH_4)_2S_2O_8$	concentration of $NaHCO_3$ (M)	reaction time (h)	rod diameter (nm)	rod length (nm)
1	2.5/1.0	0.05	12	20	200−400
2	5.0/1.0	0.05	12	50	200
3	5.0/1.0	0.10	24	60	200−300

color of the film became deep blue, the copper foil was taken out of the solution, rinsed with water and ethanol, and dried in air. The reaction conditions are summarized in Table 1.

For the synthesis of rodlike structures of $Cu_2(OH)_2CO_3$ on copper foils, the procedures are similar; the main difference is that NaOH was replaced by $NaHCO_3$. Sample 3 was prepared as follows. A solution was prepared in a 100-mL glass bottle by mixing 2 mL of the $NaHCO_3$ solution, 2 mL of the $(NH_4)_2S_2O_8$ solution (0.20 mol dm^{-3}), and 16 mL of water. The total solution volume was kept at 20 mL. A piece of copper foil ($10 \times 3.0 \times 0.25$ mm^3) was ultrasonically cleaned in acetone and then in deionized water before being immersed in the solution. In 24 h, a faint blue color appeared on the copper foil surface. Finally, the copper foil was taken out of the solution, rinsed with water and ethanol, and dried in air. Table 2 records the reaction conditions.

Characterization. X-ray diffraction (XRD) analysis was performed on a Philips PW 1830 X-ray diffractometer with a 1.5405-Å Cu Kα rotating anode point source. The source was operated at 40 kV and 40 mA, and the Kβ radiation was eliminated using a nickel filter. Transmission electron microscopy (TEM) measurements were conducted with Philips CM20 and JEOL2010 transmission electron microscopes using an accelerating voltage of 200 kV. The compound films on copper foils were transferred to carbon films on copper grids by allowing them to touch and then slide gently relative to each other. The morphologies of the compound films grown on copper foils were observed on a JEOL JSM-6300F scanning electron microscope (SEM) at an accelerating voltage of 10 kV. To prevent charging, a thin film of gold was sputtered on the sample surface. For X-ray photoelectron spectroscopy (XPS), a Physical Electronics PHI 5600 multitechnique system was used with a monochromatic Al Kα X-ray source. FTIR measurements were performed on powder samples, which were obtained by scrapping off the copper compound films from the copper surfaces, followed by mixing with KBr powder. Background correction was made using a blank KBr pellet as the reference. Thermal analysis was conducted on a TGA/DTA 92 Setaram II thermal analyzer; the samples were heated from room temperature to 1100 °C at a rate of 5 °C/min in a steady flow of dry N_2 (20 mL/min).

Results and Discussion

I. Control of the Product Composition and Nanostructure. When the reaction was carried out in acidic solution (pH < 10), no film was deposited on the copper surface. Instead, copper was continuously oxidized and dissolved, forming a blue solution. By using pH 8−10 and [NaOH]/[$(NH_4)_2S_2O_8$] = 0.5−1.5, a light-blue powder precipitated on the bottom and the inside wall of the glass bottle. The copper foil lost its metallic luster, but there was no perceptible solid deposit on it. The final solution is almost colorless, indicating that most Cu^{2+} ions from the surface oxidation have been precipitated. The XRD pattern of a precipitate sample is shown in Figure 1A, which matches the powder diffraction pattern of monoclinic $Cu_4(SO_4)(OH)_6$ (JCPDS card 43-1458) well. The precipitate consists of spindle-shaped sheets (SEM image in Figure 1B). Figure 1C shows the TEM image of a single sheet, and the inset is the corresponding electron diffraction pattern, from which a

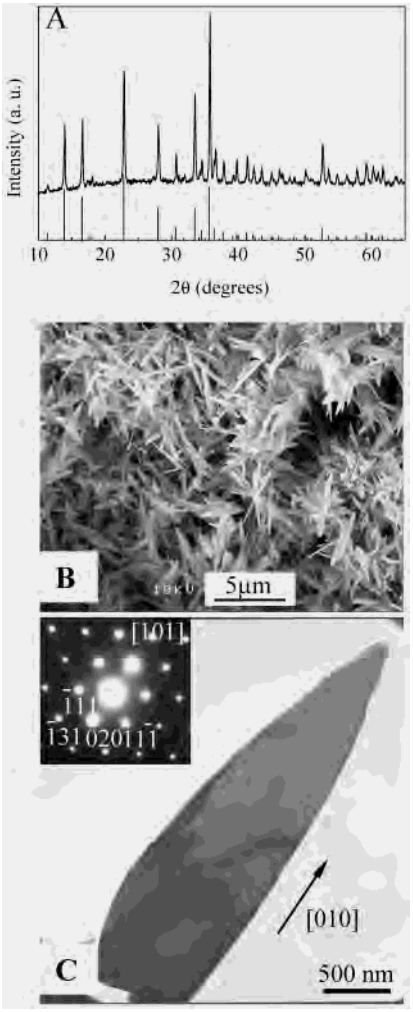

Figure 1. XRD profile (A), SEM image (B), and TEM image (C) of the $Cu_4(SO_4)(OH)_6$ precipitate obtained at pH 9, [NaOH]/[$(NH_4)_2S_2O_8$] = 1:1, and reaction time = 24 h. Inset of (C): SAED pattern from a single sheet of $Cu_4(SO_4)(OH)_6$. The vertical lines in A represent the standard powder diffraction pattern of the corresponding bulk material (JCPDS card 43-1458).

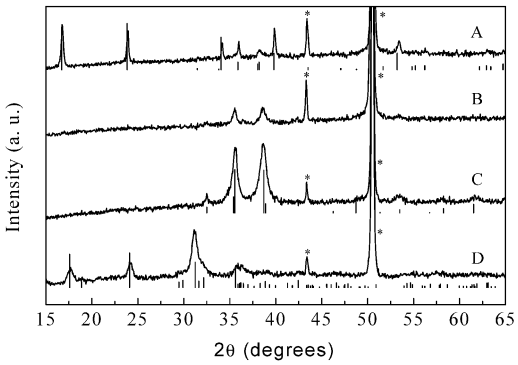

Figure 2. XRD patterns of the compound films on copper foil: (A) $Cu(OH)_2$ fibers prepared after reaction for 9.0 h with [NaOH] = 1.25 M and $[NaOH]/[(NH_4)_2S_2O_8] = 25:1$; (B) CuO sheets prepared after reaction for 12 h with [NaOH] = 1.0 M and $[NaOH]/[(NH_4)_2S_2O_8] = 5:1$; (C) CuO sheets and whiskers prepared after reaction for 12 h with [NaOH] = 5.0 M and $[NaOH]/[(NH_4)_2S_2O_8] = 25:1$; (D) $Cu_2(OH)_2CO_3$ rod arrays prepared after reaction for 24 h with $[NaHCO_3] = 0.1$ M and $[NaHCO_3]/[(NH_4)_2S_2O_8] = 5:1$. Peaks marked with * are from the copper substrate. Vertical lines represent the standard powder diffraction patterns of the corresponding bulk materials (JCPDS cards 13-0420, 48-1548, and 41-1390).

single-crystal structure is manifest. Here, the zone axis is [101], and the [010] axis is along the spindle direction. The structure of the monoclinic $Cu_4(SO_4)(OH)_6$ is also supported by a FTIR spectrum of the $Cu_4(SO_4)(OH)_6$ sample, which shows four hydroxyl ion bands at 3588, 3565, 3391, and 3277 cm^{-1} and two bands of the sulfate group at 1128 and 1087 cm^{-1}.[43] In addition, our S 2p XPS spectrum of $Cu_4(SO_4)(OH)_6$ exhibits a peak at 169.0 eV ($2p_{3/2}$),[44] indicating the presence of the sulfate group.

$Cu(OH)_2$ Fibers and Scrolls Assembled on a Copper Surface. By increasing the molar ratio of $[NaOH]/[(NH_4)_2S_2O_8]$ to >10 and the concentration of [NaOH] to >1 M, the above reaction leads to the deposition of a blue film on the copper foil. Figure 2A displays the XRD pattern of the blue film prepared at a relatively low concentration of NaOH (1.25 M). All of the diffraction peaks can be indexed to the orthorhombic phase of $Cu(OH)_2$ (space group: $Cmc2_1$),[32,33] except those marked with "*" from the copper substrate. The broadening at the leading edge of (111) and the falling edge of (022) indicates the presence of a small amount of CuO due perhaps to the dehydration of $Cu(OH)_2$. The calculated cell parameters are $a_0 = 2.946$ Å, $b_0 = 10.544$ Å, and $c_0 = 5.238$ Å, which are in reasonable agreement with the corresponding literature values: $a_0 = 2.9471$ Å, $b_0 = 10.5930$ Å, and $c_0 = 5.2564$ Å. As shown in Figure 3, the blue film contains mainly fibers of $Cu(OH)_2$. With a reaction time of 0.50 h, the fibers were distributed on the copper foil like bunches of straws (Figure 3A). After reacting for 9.0 h, the fibers became much more dense and thicker (Figure 3B). A close examination of the SEM image reveals bundle morphologies of fibers (Figure 3C) with diameters of ~30−100 nm (Figure 3D). The ED pattern in the inset of Figure 3D obtained from a seemingly single fiber (see arrow) suggests that the fiber may be made of twin crystals. For a reaction time longer than 10 h, the blue film on the copper substrate

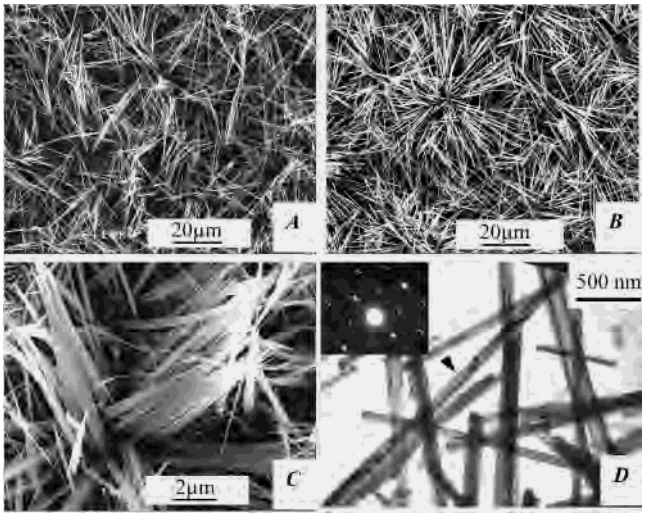

Figure 3. SEM images of $Cu(OH)_2$ fibers grown on copper foil at [NaOH] = 1.25 M and $[NaOH]/[(NH_4)_2S_2O_8] = 25:1$ after reacting for 0.5 h (A) and 9.0 h (B). (C) Higher magnification of B. (D) TEM images of the sample shown in B. Inset: SAED pattern of a single fiber shown in D with an arrow.

became increasingly black owing to the transformation of $Cu(OH)_2$ to sheetlike CuO, as will be described below.

When the concentration of NaOH was increased further to >2.0 M, the fibers of $Cu(OH)_2$ generally became thicker, accompanied by the appearance of some interesting morphologies as shown in Figure 4. The fibers are well separated from each other (Figure 4A) with diameters >100 nm when the reaction time was 20 min. The flatness of the tip sections indicates that the fibers are solid (Figure 4B). With a longer reaction time (~1.0−1.5 h), the copper surface was covered compactly and uniformly with the fibers (Figure 4C). More interestingly, the fiber tips exhibit clear open structures (Figure 4D). Careful examination at higher magnifications (Figure 4E and F) reveals more details of the tubular fiber tips. Parts G and H of Figure 4 show, respectively, a rolled layer not yet closed and irregularly broken tube tips exposing the hollow cores (see the arrows). The thickness of the tube walls is estimated to be a few tens of nanometers on the basis of the SEM images in Figure 4E and F. As discussed below, the formation of the scrolls is directly related to the dehydration stage of the $Cu(OH)_2$ fibers. The scrolls were readily obtained in the highly basic solutions and with a sufficient reaction time.

Figure 5A shows the TEM image of a single fiber from a sample used in Figure 4A and B. The fiber has a diameter of 150 nm. The inset gives the corresponding selected-area electron diffraction (SAED) pattern, which demonstrates that the fiber is a single crystal lying on the (001) plane and extending along the [100] direction. Presented in Figure 5B−D are TEM images of the same sample used for Figure 4C and D. In Figure 5B, a scroll is formed by rolling a sheet from the two opposite sides. The corresponding SAED pattern (inset) shows that the scroll grows along the [100] direction. Figure 5C shows clearly a scroll that was formed by rolling a sheet. The contrast between the side edges and the central portion in the upper section of the scroll reveals

(43) Degenhardt, J.; McQuillan, A. J. *Langmuir* **1999**, *15*, 4595.
(44) Watanabe, M.; Tamita, M.; Ichino, T. *J. Electrochem. Soc.* **2001**, *148*, B522.

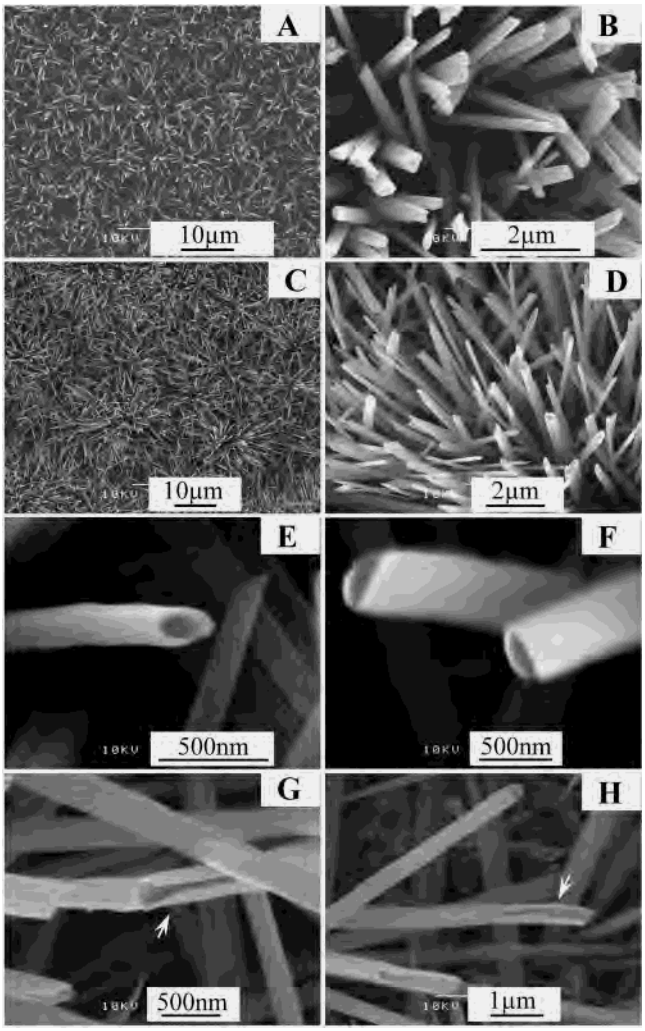

Figure 4. SEM images of $Cu(OH)_2$ fibers (A, B; reaction time = ~20 min) and scrolls (C−H; reaction time = 1.0 h) grown on copper foil at [NaOH] = 2.5 M and $[NaOH]/[(NH_4)_2S_2O_8] = 25:1$.

the hollow structure. An electron diffraction (ED) pattern of the central part is shown in the inset of Figure 5C, which is similar to that in Figure 5B except that the discrete diffraction spots are more obvious. We have also taken a HRTEM image at the side edge of the scroll in Figure 5B. Parallel fringes with a spacing of 5.4 Å, which corresponds to the spacing of the (020) planes, can be identified. This is consistent with the rolling of (020) sheets into scrolls.

As a brief summary, the growth of fiber and scroll films of $Cu(OH)_2$ can be controlled by varying the concentration of NaOH and the reaction time if $[NaOH]/[(NH_4)_2S_2O_8]$ is in the range of 10−40 (Table 1). If the concentration of NaOH is lower than 2.0 M, then thin fibers of $Cu(OH)_2$ can be formed in a broad time window (0.10−9.0 h); a longer reaction time results in the formation of black CuO sheets. For [NaOH] > 2.0 M, however, fibers of $Cu(OH)_2$ can be obtained only when the reaction time is less than 1.0 h. During a short reaction time period (1.0−1.5 h), films of $Cu(OH)_2$ scrolls are obtained. With even longer reaction times, they change to black CuO sheets.

Hierarchical Structures of CuO Sheet Films. It is noteworthy that the synthetic procedures described above

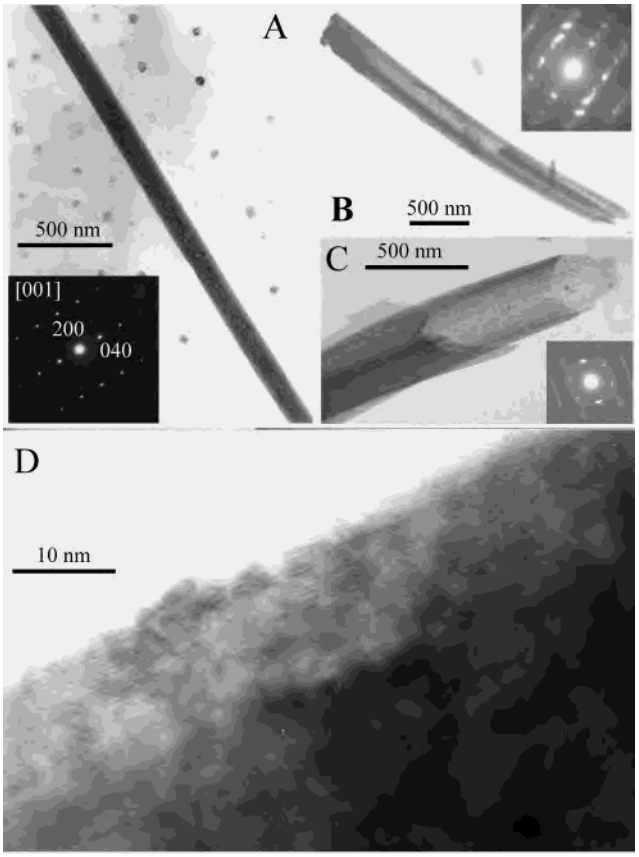

Figure 5. (A) TEM image of a $Cu(OH)_2$ fiber as in Figure 4A and B. (B−D) TEM images of the same samples as used for Figure 4C and D. (B) A scroll is formed by curling the two opposite sides of a sheet. Inset: SAED pattern of the scroll. (C) HRTEM image of a closed scroll. Inset: SAED pattern of the scroll. (D) HRTEM image of the scroll in B taken around the side edge.

eventually lead to the formation of CuO nanostructures for sufficiently long reaction times at pH > 10 (Table 1). When [NaOH] > 0.1 M and the molar ratio of NaOH to $(NH_4)_2S_2O_8$ was increased (from 1:2 to 2:1), the solution became blue and the blue precipitate of $Cu_4(SO_4)(OH)_6$ diminished drastically. It seems that the blue powder has largely been dissolved in the highly alkaline solution. With pH ~10−13 and $[NaOH]/[(NH_4)_2S_2O_8]$ in the range of 2:1 and 4:1, black CuO films were formed from $Cu(OH)_2$ but did not adhere well on copper surface, precipitating easily into solution. Under the conditions of pH ~13−14 and $[NaOH]/[(NH_4)_2S_2O_8]$ between 4:1 and 25:1, a slightly blue film of $Cu(OH)_2$ was formed on copper, which turned quickly (in 0.5 h) to a uniform film of low-dimensional CuO.

As mentioned above, for [NaOH] = 1.0−5.0 M and $[NaOH]/[(NH_4)_2S_2O_8]$ in the range of 5.0−50, a blue film of $Cu(OH)_2$ fibers and scrolls on copper was easily obtained. This blue film turned black in ~10 h, signifying the formation of CuO. Figure 2B shows the XRD pattern of such a black film. The observed diffraction peaks can all be indexed to monoclinic CuO (JCPDS card 48-1548). The CuO film is composed of small pieces of sheets according to the SEM image in Figure 6A. The ED pattern is the same as that shown in Figure 7C, manifesting single crystallinity. The gradual transformation of $Cu(OH)_2$ scrolls to CuO sheets was normally observed after reaction for >1.5 h when [NaOH]

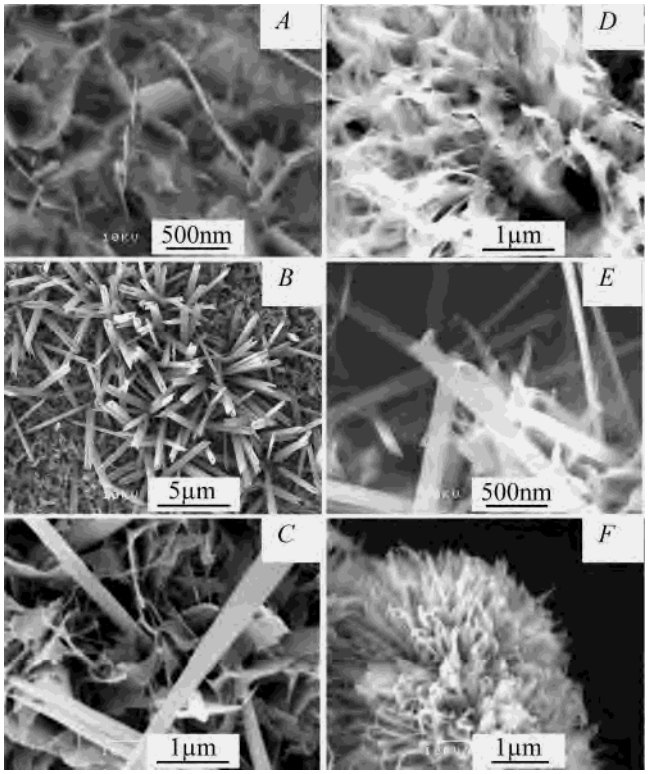

Figure 6. SEM images of CuO films. (A) Sheetlike CuO film (from the same sample as used in Figure 2B). (B, C) Blue and black regions of a film on copper foil with $Cu(OH)_2$ scrolls and CuO sheets coexistent, which was prepared at [NaOH] = 2.5 M and $[NaOH]/[(NH_4)_2S_2O_8] = 25:1$ after reacting for 1.5 h. (D) Sheet/whiskerlike CuO film (from the same sample as used in Figure 2C). (E, F) Blue and black regions of a film prepared under the same conditions as in D except with a reaction time of 1.5 h.

= 2.5 M. Parts B and C of Figure 6 show SEM images of a sample during the transformation in the blue and black areas, respectively. Both tubes and sheets can be seen in Figure 6B, and the tubes are apparently shortened compared with those in Figure 4D. After further transformation, the copper surface was uniformly covered by the CuO sheets with only some remnants of the tubes (Figure 6C).

When [NaOH] was increased to the range of 5.0−7.0 M while keeping $[NaOH]/[(NH_4)_2S_2O_8] = 5.0-50$, a similar blue-to-black film transformation was also observed. However, the transformation time was shortened to 0.50−1.5 h, and the morphology of the black film was altered significantly. Figure 2C shows the XRD pattern of the CuO film prepared with 5.0 M NaOH and $[NaOH]/[(NH_4)_2S_2O_8] =$ 25:1 after reacting for 12 h. As expected, the diffraction peaks are consistent with those of monoclinic CuO (JCPDS card 48-1548). The SEM image of this film (Figure 6D) shows longer strips (or belts) of CuO with sharper tips instead of sheetlike CuO obtained at lower concentrations of NaOH. This can be seen more clearly from the TEM images in Figure 7. With a reaction time of 24 h, the belt-like morphology is apparent with widths of 30−120 nm and lengths of several micrometers (Figure 7A). Shown in Figure 7B is a typical CuO belt with a width of 60 nm, which has been broken during sample transfer. The corresponding SAED pattern (Figure 7C) along the [001] zone axis demonstrates that the belt is a single crystal with a growth direction of $[1\bar{1}0]$ (see arrow). This is corroborated by the HRTEM image in Figure 7D. From Figure 7A, one also notices the thin whiskers grown near the belt tips (see arrows). As the reaction time is extended to 72 h, such CuO whiskers grow more dense and longer with diameters of 20−50 nm (Figure 7E). Figure 7F shows the TEM image of a representative whisker with a thickness of ~20 nm. The SAED pattern (Figure 7G) reveals only the planes, which are perpendicular to the [100] growth direction. Further evidence for the whisker growth direction of [100] is given by the HRTEM image in Figure 7H (see the arrow).

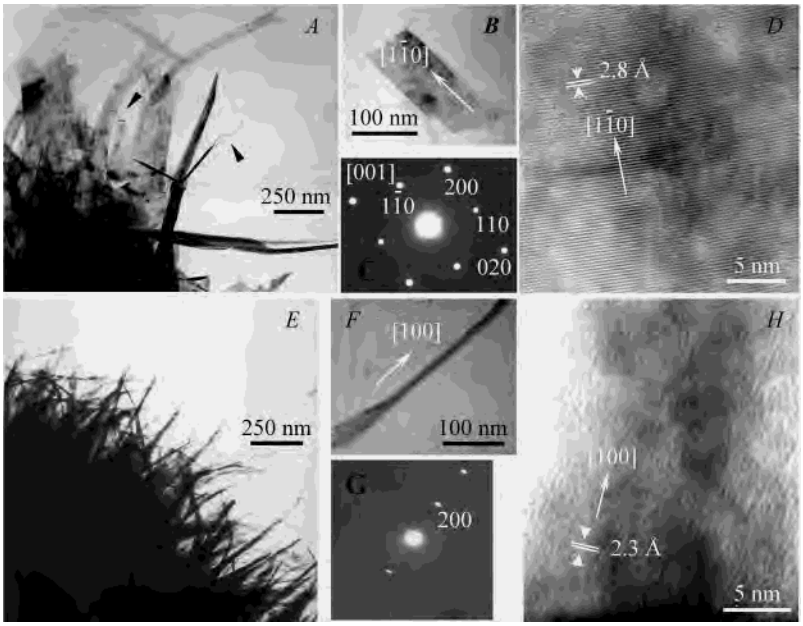

Figure 7. (A) TEM image of belt-like CuO grown on copper foil at [NaOH] = 5.0 M and $[NaOH]/[(NH_4)_2S_2O_8] = 25:1$ after reacting for 24 h. (B) TEM image of a broken piece of a CuO belt shown in A. (C) SAED pattern of B. (D) HRTEM image of B. (E) TEM image of whiskerlike CuO grown on copper foil at [NaOH] = 5.0 M and $[NaOH]/[(NH_4)_2S_2O_8] = 25:1$ after reacting for 72 h. (F) TEM image of a single CuO whisker. (G) SAED pattern of F. (H) HRTEM image of F.

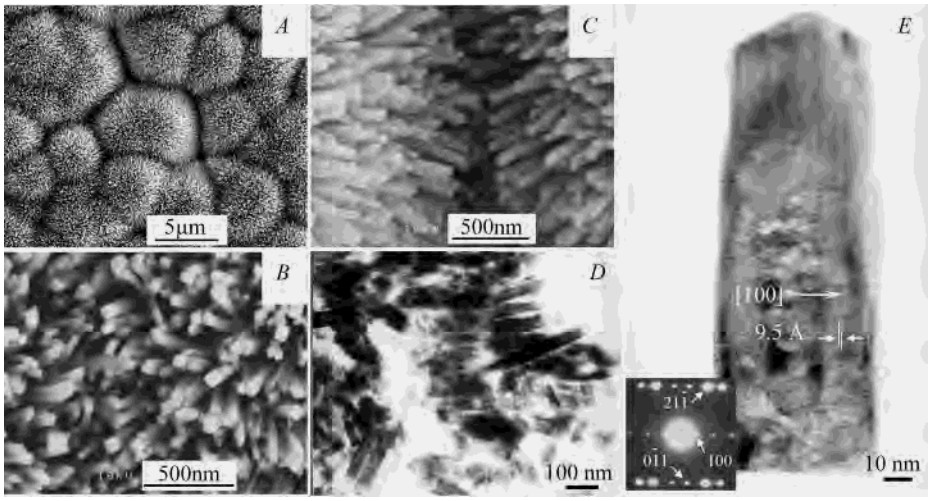

Figure 8. SEM and TEM images of the radially aligned rod pattern of $Cu_2(OH)_2CO_3$ (sample 3), which was prepared at $[NaHCO_3] = 0.1$ M and $[NaHCO_3]/[(NH_4)_2S_2O_8] = 5:1$ after reacting for 24 h. (A) Large-area SEM image. (B) Top-view SEM image. (C) Side-view SEM image. (D) TEM image. (E) HRTEM of a single rod. Inset: SAED pattern of the rod.

The coexistence of $Cu(OH)_2$ scrolls and CuO belts during the above transformation has also been observed with a reaction time of 1.5 h. In the blue areas of the film, as shown in Figure 6E, there are still plenty of tubes, but striplike sheets seem to be spit out from the tube tips. In the black areas (Figure 6F), however, the $Cu(OH)_2$ scrolls have completely changed into a hierarchical flower pattern composed of CuO belts with whiskers extending from the tips.

$Cu_2(OH)_2CO_3$ Rod Arrays. On replacing NaOH with $NaHCO_3$ and under appropriate conditions (Table 2), the procedures described above lead to the gradual growth of a faint bluish film on copper. The XRD peaks of the film (Figure 2D) can all be indexed to monoclinic $Cu_2(OH)_2CO_3$ (JCPDS card 41-1390) except for the two peaks from the copper substrate (*). In general, the $Cu_2(OH)_2CO_3$ rod films grow much more slowly on copper than the $Cu(OH)_2$ fibers and scrolls. Part of the reason is that a low concentration (0.05−0.10 M) of $NaHCO_3$ is preferred for the growth of the $Cu_2(OH)_2CO_3$ rod arrays. The rod lengths and diameters depend on the concentration of $NaHCO_3$, the molar ratio of $NaHCO_3$ to $(NH_4)_2S_2O_8$, and the reaction time, as can be seen from Table 2.

Figure 8 displays SEM and TEM images of a $Cu_2(OH)_2CO_3$ rod film prepared at $[NaHCO_3] = 0.10$ M (sample 3 in Table 2). The $Cu_2(OH)_2CO_3$ rods are radially aligned like flowers (Figure 8A), which cover the copper surface uniformly and compactly. The cross sections of the rods are square or rectangular and have a nearly monodispersed dimension of <100 nm (Figure 8B). From the flower edges (Figure 8C), the rod lengths are estimated to be several hundred nanometers. The TEM image in Figure 8D shows that the rods are actually somewhat thinner than those in the SEM images. Shown in Figure 8E is a HRTEM image of a single $Cu_2(OH)_2CO_3$ rod that is ~60 nm thick and ~150 nm long. The rod is clearly a single crystal, and lattice fringes are observed parallel to the length direction with a spacing of 9.5 Å, which well matches the spacing between the {100} planes. This is consistent with the SAED pattern (inset of Figure 8E) along the [011] axis. The growth direction of the rods appears to be $[12\bar{2}]$.

When the concentration of $NaHCO_3$ is decreased to 0.05 M (sample 2 in Table 2), the film was found to have similar morphologies except that the rods are thinner and shorter. By maintaining $[NaHCO_3]$ and decreasing the molar ratio of $[NaHCO_3]$ to $[(NH_4)_2S_2O_8]$ (sample 1 in Table 2), the rods became even thinner but longer with poorer crystallinity. Therefore, low concentrations of $NaHCO_3$ are conducive to the growth of long, thin $Cu_2(OH)_2CO_3$ rods, and to improve rod crystallinity, high molar ratios of $[NaHCO_3]$ to $[(NH_4)_2S_2O_8]$ are required.

II. Spectroscopic and Thermochemical Characterization. FTIR, XPS, and Auger spectra of the materials described above have been recorded (Supporting Information). Characteristic vibrational bands and core-level structural features have been obtained for the copper compound films. These data not only provide further evidence of the nanostructures but also verify their compositional purity.

For thermal analysis, the films of $Cu(OH)_2$, CuO, and $Cu_2(OH)_2CO_3$ were peeled off the copper substrates using a stainless steel spatula. The thermogravimetric analysis−differential thermal analysis (TGA−DTA) curves are shown in Figure 9. For the $Cu(OH)_2$ fiber sample (Figure 9A), two distinct endothermic peaks appear at 156.84 and 845.35 °C in the DTA curve; correspondingly, two weight-loss steps are detected around these temperatures in the TGA curve. From XRD analysis and weight-loss calculations, the low-temperature peak is associated with the loss of structural H_2O, and the high-temperature peak marks the conversion of CuO to Cu_2O. Bulk CuO was reported to decompose to Cu_2O and O_2 at 1030 °C at atmospheric pressure in air,[34] which is significantly higher than the decomposition temperature of the present nanoscale CuO. The results from the TGA−DTA analysis of the $Cu(OH)_2$ scrolls are similar. It is noteworthy that this experiment shows no sign of encapsulated water in the scrolls.

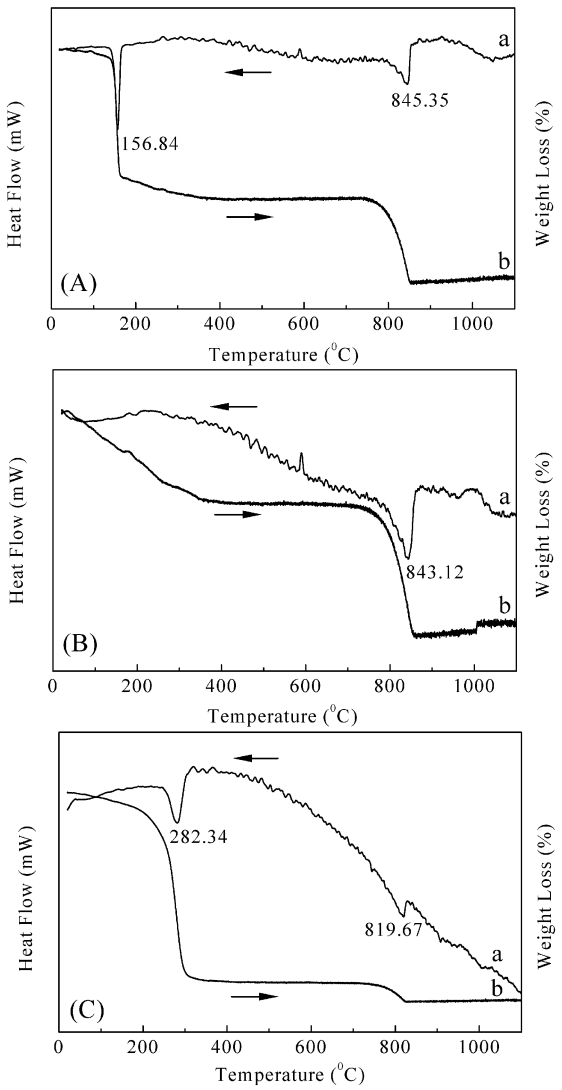

Figure 9. DTA (a)−TGA (b) curves of (A) $Cu(OH)_2$ fibers (from the same sample as used in Figure 2A); (B) CuO sheets (from the same sample as used in Figure 2B); and (C) $Cu_2(OH)_2CO_3$ rods (from the same sample as used in Figure 2D).

DTA of the CuO sheet sample exhibits only one endothermic peak at 843.12 °C, whereas the TGA curve has a sluggish weight-loss region from room temperature to ~350 °C and a sharper weight-loss step at 843 °C (Figure 9B). The sharp weight-loss step is due to the conversion of CuO to Cu_2O as established by XRD analysis and weight-loss calculations, and the sluggish weight loss may be caused by the so-called buoyancy effect during the heating process.

For the rods of $Cu_2(OH)_2CO_3$, two endothermic peaks along with the weight-loss features at 282.34 and 819.67 °C are identified in the DTA curve and the TGA curve, respectively (Figure 9C). XRD analysis and weight-loss calculations suggest the decomposition of $Cu_2(OH)_2CO_3$ to CuO at 282.34 °C. This is comparable to the decomposition of bulk $Cu_2(OH)_2CO_3$ (~280 °C).[34] The high-temperature peak corresponds to the conversion of CuO to Cu_2O, which is still substantially lower than those in Figure 9A and B due largely to the smaller sizes of the $Cu_2(OH)_2CO_3$ rods. SEM observation shows that the morphology of the $Cu_2(OH)_2CO_3$ rods does not change significantly at ~300 °C in N_2 (for 1.5 h). Bulk CuO decomposes to Cu_2O and O_2 at 1030 °C at atmospheric pressure in air.[34]

III. Mechanistic Aspects. In acidic and weak alkaline solutions, $(NH_4)_2S_2O_8$ oxidizes and dissolves copper continuously, preventing films from being formed on the copper surface. The Cu^{2+} ions resulting from copper oxidation react with OH^- ions as well as excess SO_4^{2-} ions from the reduction of $(NH_4)_2S_2O_8$, forming a blue precipitate of $Cu_4(SO_4)(OH)_6$.

$$4Cu + 14OH^- + 4(NH_4)_2S_2O_8 \rightarrow Cu_4(SO_4)(OH)_6 + 7SO_4^{2-} + 8NH_3\uparrow + 8H_2O \quad (1)$$

This is also the case when a small amount of NaOH is added to a solution containing excess $CuSO_4$, whereby a blue $Cu_4(SO_4)(OH)_6$ precipitate forms instead of $Cu(OH)_2$. The reason is that the solubility product of $Cu_4(SO_4)(OH)_6$ has reached the precipitation limit before that of $Cu(OH)_2$. The spindlelike morphology of the $Cu_4(SO_4)(OH)_6$ crystallites is related to the strong bonds of $>Cu(OH)_2<$ chains and weaker $-OH...OSO_3^{2-}$ bonds, which cause the platelet structure to orient along [010].[32]

As can be seen in Table 1, at $14 > pH > 10$ and $2.0 < [NaOH]/[(NH_4)_2S_2O_8] < 25$ or $5.0\ M < [NaOH] < 7.0\ M$ and $5.0 < [NaOH]/[(NH_4)_2S_2O_8] < 50$, a faint blue film briefly appears on the copper surface and is quickly transformed to a brown or black CuO film. When [NaOH] is raised to 1.0−5.5 M and $[NaOH]/[(NH_4)_2S_2O_8]$ is maintained at 10−40, the blue $Cu(OH)_2$ film is readily formed on copper and can last for a much longer time. However, with the lapse of time, the blue $Cu(OH)_2$ is eventually dehydrated to form black CuO. The reactions are summarized as follows.

$$Cu + 4OH^- + (NH_4)_2S_2O_8 \rightarrow Cu(OH)_2 + 2SO_4^{2-} + 2NH_3\uparrow + 2H_2O \quad (2)$$

$$Cu(OH)_2 \rightarrow CuO + H_2O \quad (3)$$

The formation of $Cu(OH)_2$ and CuO nanostructures on copper surfaces involves inorganic polymerization (polycondensation) reactions under alkaline and oxidative conditions. Particle morphology may vary depending on synthetic conditions. Even aging in aqueous solution may bring about significant dimensional, morphological, and structural changes, as have been noticed by Matijević and co-workers.[32] The orthorhombic $Cu(OH)_2$ consists of (olated) chains in the (001) planes, which are oriented along [100] and characterized by the square-planar coordination of the Cu^{2+} ions with strong $\sigma_{x^2-y^2}$ bonds. The Cu^{2+} ions form two other longer and more ionic bonds with two OH^- groups from neighboring chains along the *c* axis, completing a deformed octahedron in the first coordination sphere of Cu^{2+}. By juxtaposing the chains in this way, one obtains a corrugated sheet parallel to (010) as shown in Figure 10. Essentially, the sheet is formed by edge sharing of the distorted $Cu(OH)_6$ octahedra. A 3D $Cu(OH)_2$ crystal is formed by the stacking of the sheets through hydrogen bonds. Presumably, the assembly of $Cu(OH)_2$ pro-

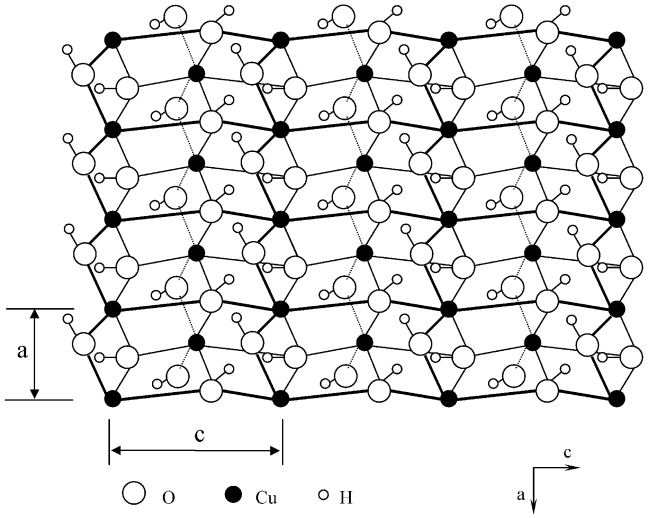

Figure 10. *ac* projection of the (010) plane of orthorhombic $Cu(OH)_2$. A corrugated layer formed by edge sharing of distorted $Cu(OH)_6$ octahedra.

ceeds through the condensation of Cu^{2+} and OH^- (olation reaction), forming μ_4-OH bridges. The OH^- ligand acts as a nucleophile and undergoes a change in coordination only when it switches from a terminal ligand in a monomer to a bridging ligand in a condensed species. According to the Bravais−Friedel−Donnay−Harker analysis,[45] the growth speed of such crystal is normally proportional to $1/d_{hkl}$. The interplane distance of (010) is the longest (10.60 Å) with relatively loose hydrogen bond linkages, whereas the interplanar distance of (100) is the shortest (2.952 Å). Therefore, the fibers and tubes grow along the [100] direction by stacking and scrolling the sheets parallel to (010), respectively.

However, when the concentration of NaOH is >2.0 M and the reaction time is longer than 1.0 h, scrolls are obtained. As we know, the 2D layers of distorted $Cu(OH)_6$ octahedra parallel to (010) are connected through H-bonds, and they are inherently asymmetric owing to the Jahn−Teller distortion. Conceivably, the highly basic condition may weaken the interlayer H-bond linkage at the sheet edges and cause stresses in the layers. Consequently, the sheets were rolled so as to relieve the stresses, forming the final tubular structure. The adsorption of NH_3 seems to be relatively unimportant because the use of the oxidant $Na_2S_2O_8$ instead of $(NH_4)_2S_2O_8$ for the synthesis of $Cu(OH)_2$ tubes gave similar results. Analogous whiskers, slender sheets, and tubes have been observed on titania by Gedanken et al. in their sonochemical experiments.[46]

As mentioned above, the blue $Cu(OH)_2$ films under a broad range of alkaline conditions are eventually changed to black CuO sheet films although at rather different time frames. In fact, the corrugated layer structure of $Cu(OH)_2$ (Figure 10) is unstable against oxolation because oxygen atoms are either pentacoordinated or tricoordinated. Consequently, it is transformed to monoclinic CuO by breaking the interplanar hydrogen bonds under certain reaction conditions such as high pH or long reaction time. The monoclinic CuO is characterized by chains of copper with the square-planar coordination of μ_4-O bridges. The cleavage of the interplanar hydrogen bonds causes the $Cu(OH)_2$ fibers and scrolls to crack into pieces of CuO sheets. This can be grasped from snapshots taken at an intermediate stage of dehydration (Figure 6B and C). Here, the dehydration of $Cu(OH)_2$ shortens the scrolls, and at the same time, sheets of CuO are formed. The bulk conversion of blue $Cu(OH)_2$ to CuO tenorite has been observed after moderate heating or at high pH when Cu(II) salt was used as a reagent.[32] A possible mechanism similar to that described above was proposed by Jolivet et al. to explain the transformation.[47]

On replacing NaOH with $NaHCO_3$ in the synthesis described above and setting the pH at 8.0−8.5 in the aqueous solution, the copper surface is covered by a blue $Cu_2(OH)_2CO_3$ rod film. The reaction is believed to go as follows:

$$2Cu + 4HCO_3^- + 2S_2O_8^{2-} \rightarrow Cu_2(OH)_2CO_3 + 4SO_4^{2-} + 3CO_2\uparrow + H_2O \quad (4)$$

The formation of the $Cu_2(OH)_2CO_3$ rod film on copper foil proceeds much more slowly than that of $Cu(OH)_2$ fiber and scroll films in aqueous solutions. One of the reasons is that a low concentration (0.05−0.10 M) of $NaHCO_3$ is favored for the synthesis of uniform rod arrays of $Cu_2(OH)_2CO_3$ on copper foil. Both the amount of oxidant $(NH_4)_2S_2O_8$ and the reaction time have an effect on the lengths and the diameters of the $Cu_2(OH)_2CO_3$ rods.

A common structural feature of the two copper basic salts $Cu_4(SO_4)(OH)_6$ and $Cu_2(OH)_2CO_3$ is the existence of a deformed octahedron centered on the Cu(II) ions because of the Jahn−Teller effect. Such a deformed octahedron stems from a structural pattern in which the four shortest bonds of Cu−OH around a Cu(II) ion yield a roughly planar $Cu(OH)_4$ unit. The latter forms olated chains by the periodic addition of the Cu(II) and OH^- species in much the same way as in the making of $Cu(OH)_2$. The olation chains interact with each other side-by-side through the remaining OH^- or oxoanions such as SO_4^{2-} and CO_3^{2-}, giving rise to a 2D layer. The layers are joined together through hydrogen bonds between the oxoanions and OH^- groups. This is probably the main reason for the tendency to form platelike $Cu_4(SO_4)(OH)_6$ and rodlike $Cu_2(OH)_2CO_3$ with a rectangular cross section. It should be mentioned that spherical particles of $Cu_2(OH)_2CO_3$ have been synthesized by Matijević et al.[32] but with an amorphous structure. A 2D framework could not be materialized in this case because the carbonate ions form strong Cu−O bonds in the (001) planes perpendicular to the >Cu-$(OH)_2$Cu< propagation direction. It is believed that the rodlike morphology of $Cu_2(OH)_2CO_3$ that we obtained is somehow related to the intraplanar strong bonds of >Cu-

(45) (a) Hartman, P. *Crystal Growth: An Introduction*; Hartman, P., Ed.; North-Holland: Amsterdam, 1973; p 3. (b) Hartman, P.; Perdok, W. G. *Acta Crystallogr.* **1955**, *8*, 49. (c) Vere, A. W. *Crystal Growth: Principles and Progress*; Dobson, P. J., Ed.; Plenum Press: New York, 1987; p 17.

(46) Zhu, Y.; Li, H.; Koltypin, Y.; Hacohen, Y. R.; Gedanken, A. *Chem. Commun.* **2001**, 2616.

(47) Jolivet, J.-P.; Henry, M.; Livage, J. *Metal Oxide Chemistry and Synthesis: From Solution to Oxide* (translated by Bescher, E.); Wiley & Sons: New York, 2000; p 53.

$(OH)_2Cu<$ and the interplanar weak hydrogen bonds of $O-H\cdots OCO_2$.

Conclusions

Nanostructured films of a series of copper compound materials have been synthesized on a copper foil by a simple liquid−solid reaction under alkaline and oxidative conditions at ambient temperature and pressure. These materials include $Cu(OH)_2$ fibers and scrolls, CuO sheets and whiskers, and $Cu_2(OH)_2CO_3$ rod arrays. The films were formed by the direct oxidation of copper in NaOH or $NaHCO_3$ aqueous solutions with an oxidant $(NH_4)_2S_2O_8$. Most of the structures are phase-pure single crystallites despite the low-temperature fabrication processes we adopted. The evolution of the film structures as a function of the solution treatment time and the concentration of NaOH aqueous solution from fibers of $Cu(OH)_2$ to scrolls of $Cu(OH)_2$ to sheets or whiskers of CuO has been demonstrated. By replacing NaOH with $NaHCO_3$ in the synthesis, uniform $Cu_2(OH)_2CO_3$ rod arrays have been successfully fabricated. The advantages of our method for the preparation of copper compound films with ultrafine structures are its simplicity, high yield, and mild reaction conditions and the ability to produce these materials as single crystals and in the form of arrays. Therefore, it offers an attractive and convenient path to the large-scale engineering of ordered inorganic nanostructures on metal electrodes.

Acknowledgment. This work was supported by an RGC grant administered by the UGC of Hong Kong. We thank the MCPF of HKUST for assistance in sample characterization.

Supporting Information Available: FTIR, XPS, and Auger spectra of the materials used in this work. This material is available free of charge via the Internet at http://pubs.acs.org.

IC0344214